Hindawi
Geofluids
Volume 2021, Article ID 9468290, 10 pages
https://doi.org/10.1155/2021/9468290

Research Article

Investigation on Damage Characteristic and Constitutive Model of Deep Sandstone under Coupled High Temperature and Impact Loads

Zhang Rongrong,[1,2,3] Yang Yi,[2,3] and Ma Dongdong[1,2,3]

[1]*State Key Laboratory of Mining Response and Disaster Prevention and Control in Deep Coal Mine, Anhui University of Science and Technology, Huainan, 232001 Anhui, China*
[2]*Research Center of Mine Underground Engineering, Ministry of Education, Anhui University of Science and Technology, Huainan, 232001 Anhui, China*
[3]*School of Civil Engineering and Architecture, Anhui University of Science and Technology, Huainan, 232001 Anhui, China*

Correspondence should be addressed to Ma Dongdong; dongdonm@126.com

Received 8 April 2021; Revised 10 June 2021; Accepted 17 June 2021; Published 30 July 2021

Academic Editor: Zhongqiong Zhang

To investigate the coupling damage characteristics of rock after high-temperature treatment under impact load, dynamic uniaxial compression tests for deep sandstone specimen under laboratory conditions varying with high temperature (i.e., 25°C, 100°C, 300°C, 500°C, 700°C, and 900°C) and strain rate (i.e., 170 s^{-1}, 205 s^{-1}, and 240 s^{-1}) were performed using splitting Hopkinson pressure bar (SHPB) system. Coupling damage variable of deep sandstone was deduced based on the Lemaitre equivalent strain theory. Moreover, the damage parameters of deep sandstone were systematically determined according to the test data, and the effects of high temperature and strain rate on damage growth curves were investigated. Finally, a dynamic compound damage constitutive model, which could consider the coupling damage, was established and verified to describe the dynamic mechanical characteristic of deep sandstone. Theoretical and experimental results indicated that the simulated stress-strain curves matched the test data well and the proposed coupling damage constitutive model could reflect the high temperature-induced weakening and strain rate strengthening effect.

1. Introduction

With the depletion of shallow resources in the earth, the proportion of deep resource mining is increasing gradually, and the effect of high temperature on the physical and mechanical properties of rock materials is becoming more and more prominent [1–3]. Moreover, the utilization and stability analysis of deep rock engineering, such as nuclear waste disposal, core drilling, geothermal resource development, and postfire reconstruction of rock mass, is closely related to the physical and mechanical behavior of rocks after high temperature [4]. In addition to high temperature, deep rock structures are inevitably subject to impact loads derived from rock burst, blasting excavation, and earthquake [5–7]. Therefore, it is of great practical importance to study the dynamic behavior of rock after different high-temperature treatments for rational design and rapid excavation in deep rock engineering.

Aiming at the influences of high temperature and impact load on physical and mechanical properties of deep rock, substantial effort has been performed by heating rock specimens to analyze the variation in macroscopic mechanical properties and microstructure and mineral composition. Many investigations have yielded valuable achievements. Sandstone has always been a hot research object in deep rock field because of its extensive existence; for instance, Li et al. [8] investigated the dynamic strength and deformation properties of coal measure sandstone after high-temperature treatment, and the thermal effect mechanism was studied using X-Ray Diffraction (XRD) and Scanning Electron Microscopy (SEM) technologies. Huang and Xia [9] heated

Longyou sandstone at four treatment temperatures (25°C, 250°C, 450°C, and 600°C), and the Computed Tomography (CT) technique was utilized to quantify the thermal damage degree of sandstone specimens. Finally, the correlation between damage variable and dynamic peak stress was established. Additionally, a larger number of impact tests were carried out to investigate the mechanical properties of post heated rock with dynamic loads exerted by the splitting Hopkinson pressure bar (SHPB) system, which had been considered an invaluable device providing dynamic loading on various materials [10–13]. Yao et al. [14] carried out dynamic impact tests on Longyou sandstone specimens subjected to temperatures with various strain rates, and test results illustrated that loading rate presented positive effect on dynamic tensile strength, while the high temperature showed negative effect. To compare the thermal-induced damage for different rock types, four types of rock were selected and subjected to high temperature from 25°C to 800°C [15], and the XRD, Differential Scanning Calorimeter (DSC), and Derivative Thermogravimetry (DTG) techniques were adopted to study their mineral compositions and microscopic damage of rock specimens. Chen et al. [16] heated sandstone specimens at the rising temperature rate of 10°C/min from 25°C to 1000°C and then naturally cooled them to room temperature. The dynamic stress-strain curves and failure modes of sandstone were systematically investigated, and test results demonstrated that the break degree increased with increasing heat temperature and impact velocity. Xu and Liu [17] found that strain rate showed enhancement effect on both peak stress and peak strain of marble specimens after high-temperature treatment, while the relation between loading rate and elastic modulus was not obvious. Finally, the mechanism of strain rate enhancement effect on dynamic mechanical properties of rock was discussed by combining with the microstructure, energy absorption, and stress state. Zhang et al. [18] studied the compound damage growth characteristic of rock materials considering the freeze-thaw and external loads. Wang et al. [19] established the statistical damage constitutive model of saturated fine-grained sandstone based on damage mechanics, and the damage growth regular of the saturated fine-grained sandstone under different confining pressures was discussed. Shan et al. [20] analyzed the characteristics of dynamic stress-strain curves of artificial frozen red sandstone and found that frozen red sandstone can be considered as a nonuniform particle composed of elastic, damage, plastic, and viscous properties based on the damage evolution and the component model theory. Finally, a time-dependent damage model which included the damaged body element, the clay pot, and the spring was established and verified. Research on damage characteristic and constitutive relationship of rock subjected to coupling high temperature and dynamic loads can help comprehend its dynamic behaviors and fracture process and hence improve stability analysis of underground excavation in deep rock engineering. However, by summarizing the experimental and numerical simulation achievements, it can be noticed that the previous works on mechanical characteristic of rock bearing coupling dynamic load and high temperature mainly give attention to strength and deformation characteristic, energy dissipation, and failure mode, while limited attempts have been made to study the damage characteristic and constitutive mode of deep rock considering the coupling thermal and dynamic damage.

This paper is organized as follows. Introduction presents the research status and engineering significance. Section 2 describes the test procedure and effects of high temperature and strain rate on physical and dynamic mechanical parameters of deep sandstone specimen according to laboratory test results. The defined method for the coupled damage variable considering both temperature and impact load is detailed in Section 3; moreover, the effects of strain rate and temperature on damage growth curves are investigated and discussed. Finally, a compound damage constitutive model based on Zhu-Wang-Tang (ZWT) model is established and verified in Section 4. Section 5 summarizes the main conclusions of this research.

2. Test Device and Result

2.1. Sample Preparation. Sandstone is the most typical rock type in the deep mining area of Huainan. In this research, deep sandstone with fine grain is collected from a deep roadway in Huainan, China. The coring machine, cutting machine, and grinding machine are used to process deep sandstone, and a diameter of 50 mm with a height of 25 mm is adopted to conduct SHPB tests [21]. Before dynamic tests, the P-wave velocity of deep sandstone specimens is tested by using a nonmetallic ultrasonic wave velocity testing system, and the samples with similar wave velocities are selected to reduce the discretion of test data. The physical and static mechanical parameters of deep sandstone are listed in Table 1.

2.2. High-Temperature Treatment and SHPB Test. The high-temperature resistance box is utilized in this test for hearing the deep sandstone specimens, and its highest value can reach 950°C. Hence, after processing and selection, 54 deep sandstone specimens are randomly separated into 6 groups and heated from room temperature to the desired temperature (i.e., 25°C, 100°C, 300°C, 500°C, 700°C, and 900°C) with the rising rate of 6°C/min, keeping the desired temperature for 4 h and then cooling naturally to room temperature. Therefore, each group has 9 specimens for conducting dynamic impact tests under various strain rates. Dynamic impact tests are conducted in State Key Laboratory of Mining Response and Disaster Prevention and Control in Deep Coal Mine, Anhui University of Science and Technology. The SHPB device is shown in Figure 1. In this test, a front pulse shaper is used to generate loading wave with longer rising time, which is beneficial for achieving stress balance inside deep sandstone specimens. After the sandstone specimens are treated well, appropriate amounts of Vaseline are applied to both sides of specimens as well as the surfaces of bars. Rock specimen is placed between the incident and transmission bars, and then, the desired impact pressure is set. Open the pressure control switch after the above steps are completed. The dynamic mechanical parameters of deep sandstone specimens are calculated using "three-wave" method [22–24].

Table 1: The physical and static mechanical parameters of deep sandstone.

Density (g/cm^3)	Porosity	P-wave velocity (m/s)	Compressive strength (MPa)	Tensile strength (MPa)
2.12	1.58%	3982	89.1	11.3

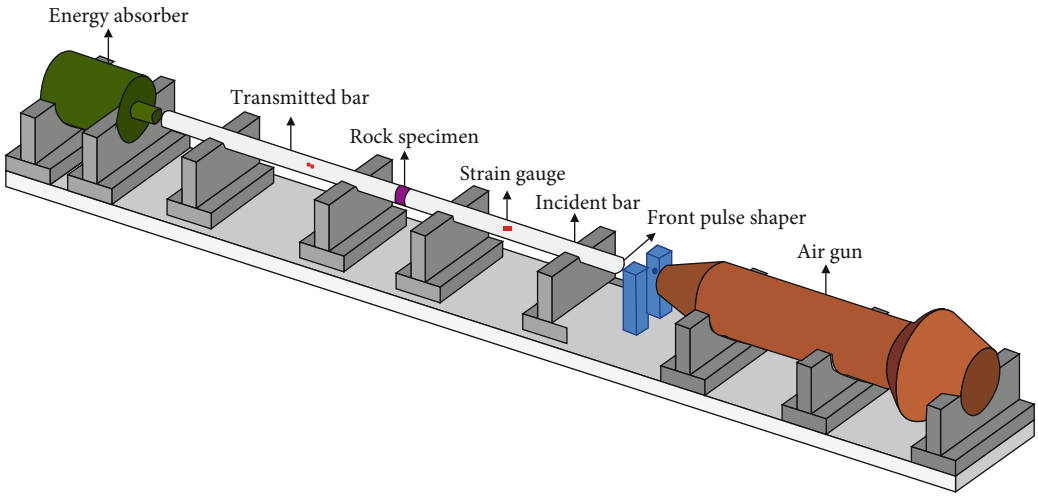

Figure 1: SHPB device.

2.3. Analysis of Test Results. For deep sandstone specimens treated with various high temperatures, the P-wave velocity and porosity are shown in Figure 2. When temperature increases from 25°C to 900°C, the P-wave velocity decreases from 3982 m/s to 2646 m/s, with a larger decrease of 33.56%, while its porosity increases by 182% after 900°C treatment compared with that at 25°C. This phenomenon is attributed to the thermal expansion of mineral particles and water vaporization of deep sandstone after high-temperature treatment, which is treated as thermal damage [25, 26]. Particularly, Jin et al. [27] investigated the inner structure and composition change of sandstone after different high-temperature treatments and found that when the temperature was higher than 500°C, the propagation of the original cracks at the boundary of different mineral particles increases and more new cracks are formed significantly due to the internal thermal stress caused by the nonuniform expansion of mineral particles. In addition, when the temperature further increased to 800°C, the crack development degree increased significantly and formed obvious crack network. Moreover, the variation rate of both wave velocity and porosity of deep sandstone specimen increases significantly after 300°C, which is caused by the loss of component and crystal water.

In SHPB test, we adjust the impact pressure to guarantee that the strain rate of specimens fluctuates in a small range. The typical dynamic stress-strain curves of deep sandstone with various high temperatures and strain rates are shown in Figure 3. It can be observed that under the same strain rate, similar characteristics are found for curves after various high temperatures, and the curve can be divided into three stages: elastic stage, plastic stage, and the postpeak failure stage. Under the same strain rate, the curve slope gradually decreases in the postpeak descent stage with the increase of

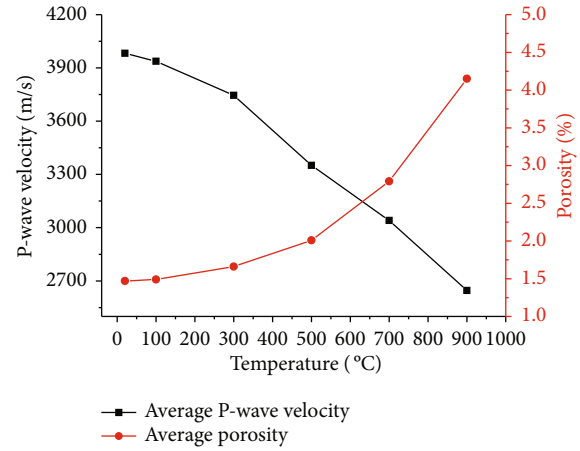

Figure 2: Variation in P-wave velocity and porosity with temperature.

temperature, indicating that the increase of temperature leads to rock failure gradually changing from brittleness to plasticity during the loading process. After the same treatment temperature, the peak stress, final strain, and peak strain increase with increasing strain rate.

In this research, the dynamic strength of deep sandstone is defined as the peak stress in the dynamic stress-strain curves, and the variation in dynamic strength of deep sandstone with strain rate and temperature is shown in Figure 4. After the same high-temperature treatment, the dynamic strength increases with the increase of strain rate, which shows obvious strain rate enhancement effect. Moreover, with increasing temperature treatment, the dynamic strengths of deep sandstone decrease gradually under the same strain rate. For instance, the dynamic strength of deep sandstone specimen after 900°C treatment is 84.45 MPa,

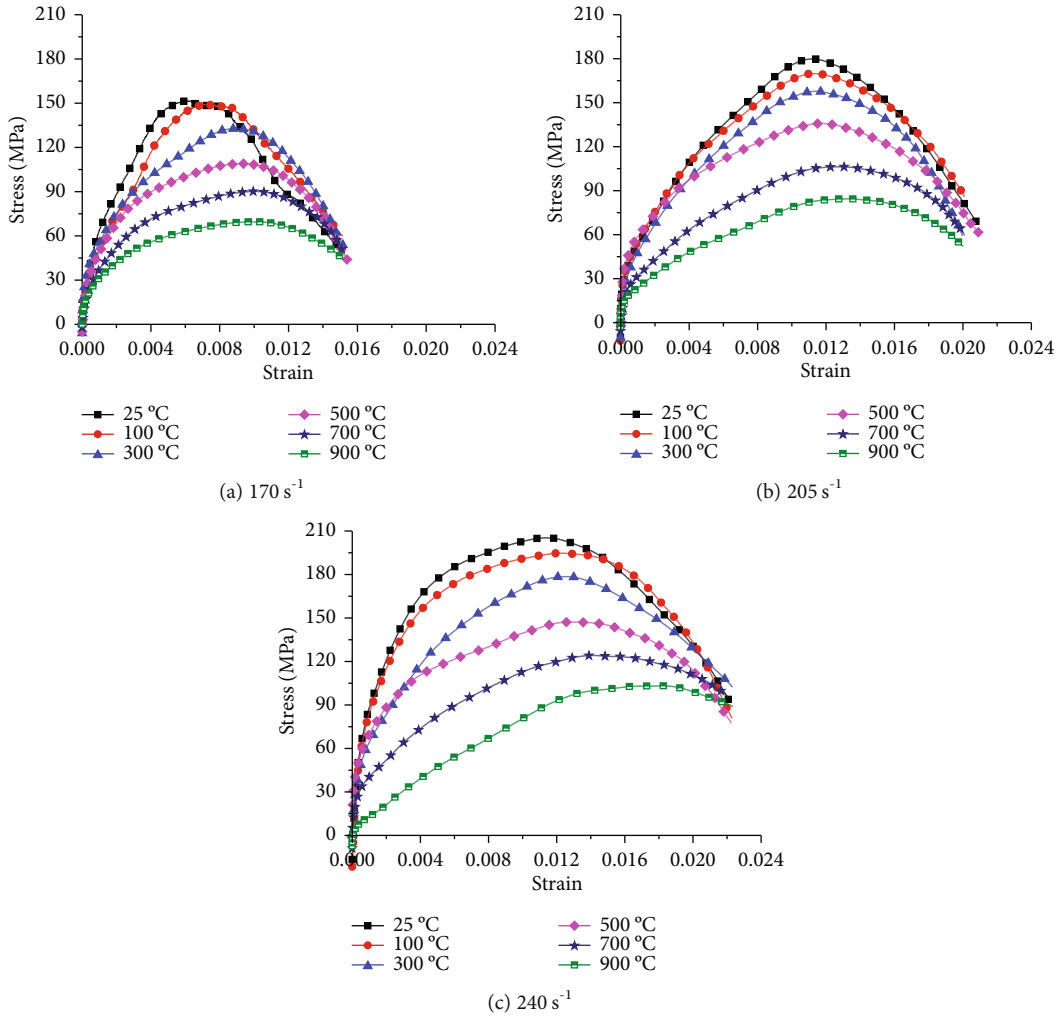

Figure 3: Dynamic stress-strain curves of deep sandstone with various strain rates.

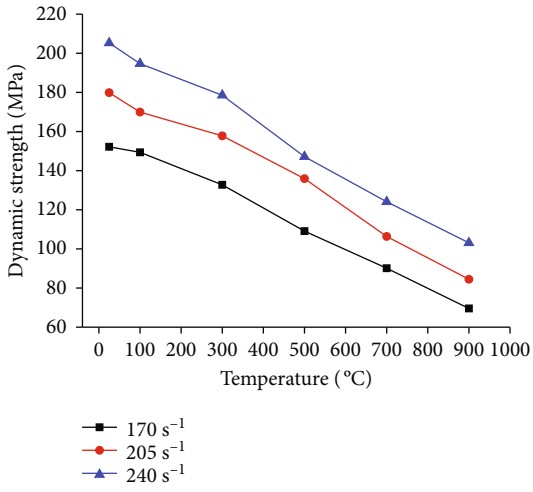

Figure 4: Variation in dynamic strength of deep sandstone with strain rate and temperature.

which is much lower than the value of 179.87 MPa after 25°C. The main mechanism for this phenomenon is likely that the thermal damage causes increases in the porosity and decreases in the wave impedance of deep sandstone specimen. Therefore, less waves can be transmitted to the transmission bar through the rock specimen under the same incident wave, resulting in the decrease of dynamic strength.

3. Damage Characteristic under Coupled High Temperature and Impact Loads

3.1. Definition Method of Coupling Damage Variable. Rock mass is cemented by a variety of mineral particles, which exists a large number of microcracks, microholes, and other defects. In addition, high temperature will inevitably lead to the generation of new cracks and the expansion of existing cracks and holes inside rock specimens. Therefore, deep sandstone specimen after high-temperature treatment is a composite damage geological material containing both thermal and native cracks, which should be considered in the definition of damage variable. In this research, the coupling damage variable is calculated based on the Lemaitre equivalent strain theory [28]. The calculation method of equivalent strain of rock specimen considering thermal damage and native damage is shown in Figure 5.

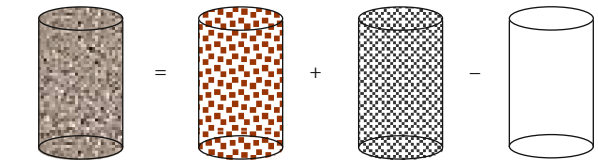

Figure 5: The calculation method of equivalent strain of rock specimen.

The coupling damage strain of rock specimen after high-temperature treatment under external load can be obtained as follows [29]:

$$\varepsilon_c = \varepsilon_t + \varepsilon_n - \varepsilon_0, \tag{1}$$

where ε_c, ε_t, ε_n, and ε_0 are the coupling damage strain, thermal damage strain, native damage strain, and no damage strain of rock specimen, respectively.

From the Lemaitre equivalent strain theory,

$$\frac{\sigma}{E_R(1-D_c)} = \frac{\sigma}{E_R(1-D_t)} + \frac{\sigma}{E_R(1-D_n)} - \frac{\sigma}{E_R}, \tag{2}$$

where σ is the stress of deep sandstone specimen; D_c, D_t, and D_n are the coupling damage variable, thermal damage variable, and native damage variable of deep sandstone specimen, respectively; and E_R is the deformation modulus of deep sandstone specimen with no damage.

From Equation (2), it can be obtained that

$$D_c = 1 - \frac{(1-D_t)(1-D_n)}{1-D_tD_n}. \tag{3}$$

Previous investigation on rock damage indicates that the variation in P-wave velocity reflects the thermal-induced damage [30, 31], and the corresponding damage variable can be calculated based on the following:

$$D_t = 1 - \left(\frac{v_n}{v_0}\right)^2, \tag{4}$$

where v_0 is the P-wave velocity of deep sandstone specimen after 25°C and v_n is the P-wave velocity of deep sandstone after different high temperatures.

For the native damage, many theoretical and laboratory test results show that the Weibull distribution can reflect the native damage evolution process of rock under dynamic load [32, 33]; the native damage variable is defined as

$$D_n = 1 - \exp\left[-\left(\frac{\varepsilon}{\lambda}\right)^n\right], \tag{5}$$

where λ and n are the material parameters of deep sandstone.

Therefore, the coupling damage variable can be obtained by substituting Equations (4) and (5) into Equation (3):

$$D_c = 1 - \frac{(v_n/v_0)^2 \exp\left[-(\varepsilon/\lambda)^n\right]}{1-\left[1-(v_n/v_0)^2\right]\left\{1-\exp\left[-(\varepsilon/\lambda)^n\right]\right\}}. \tag{6}$$

3.2. Damage Growth Characteristic of Deep Sandstone. From Equation (6), it can be noted that the damage growth curve of deep sandstone can be obtained after determining the parameters v_0, v_n, n, and λ. The values of v_0 and v_n can be confirmed from test results, as shown in Figure 2. In addition, parameters n and λ control the peak strain and the failure speed of dynamic stress-strain curves, which can be obtained by curve fitting in dynamic stress-strain curves. The damage growth curves of deep sandstone specimen with various temperatures are shown in Figure 6.

Figure 6 illustrates that there exists initial damage before dynamic loads in the curves, and its value increases with increasing temperature treatment. This phenomenon indicates that the damage growth curves have considered the thermal-induced damage caused by high-temperature treatment. Moreover, from the proportion of thermal damage, it can be found that the high-temperature thermal damage to deep sandstone specimen is relatively small when the temperature is less than 300°C, which has been observed and investigated in previous research for rock materials [34]. After 900°C treatment, the thermal-induced damage accounts for 55.8% of the total damage; the value shows that the thermal damage of deep sandstone specimen is great and its bearing capacity is greatly reduced after subjecting to relatively high temperature. With the increase of the deformation of deep sandstone specimen, the coupling damage of deep sandstone specimen gradually accumulates, and it presents "slow-fast-slow" three-stage characteristic. Moreover, its growth rate decreases with the increase of thermal damage under various strain rates.

Figure 7 displays the dynamic damage growth curves of deep sandstone specimen under different strain rates. After the same high-temperature treatment, the damage growth process of deep sandstone shows significant strain rate sensitivity. Specifically, with the increase of strain rate, the increasing rate of dynamic damage decreases gradually. This phenomenon indicates that the strain required for reaching failure state at relatively low strain rate is smaller compared with that at high strain rate. A large number of laboratory experiment date show that rock materials have obvious strain rate effect, and both the peak strain and failure strain increase with increasing strain rate [35–37], which causes the occurrence of the above phenomenon.

4. Dynamic Compound Damage Constitutive Model

4.1. Establishment of Dynamic Compound Damage Constitutive Model. The dynamic constitutive relationship of rock has always been a hot topic in rock dynamics research. Theoretical and test result indicate that the ZWT constitutive model can well reflect the dynamic strength

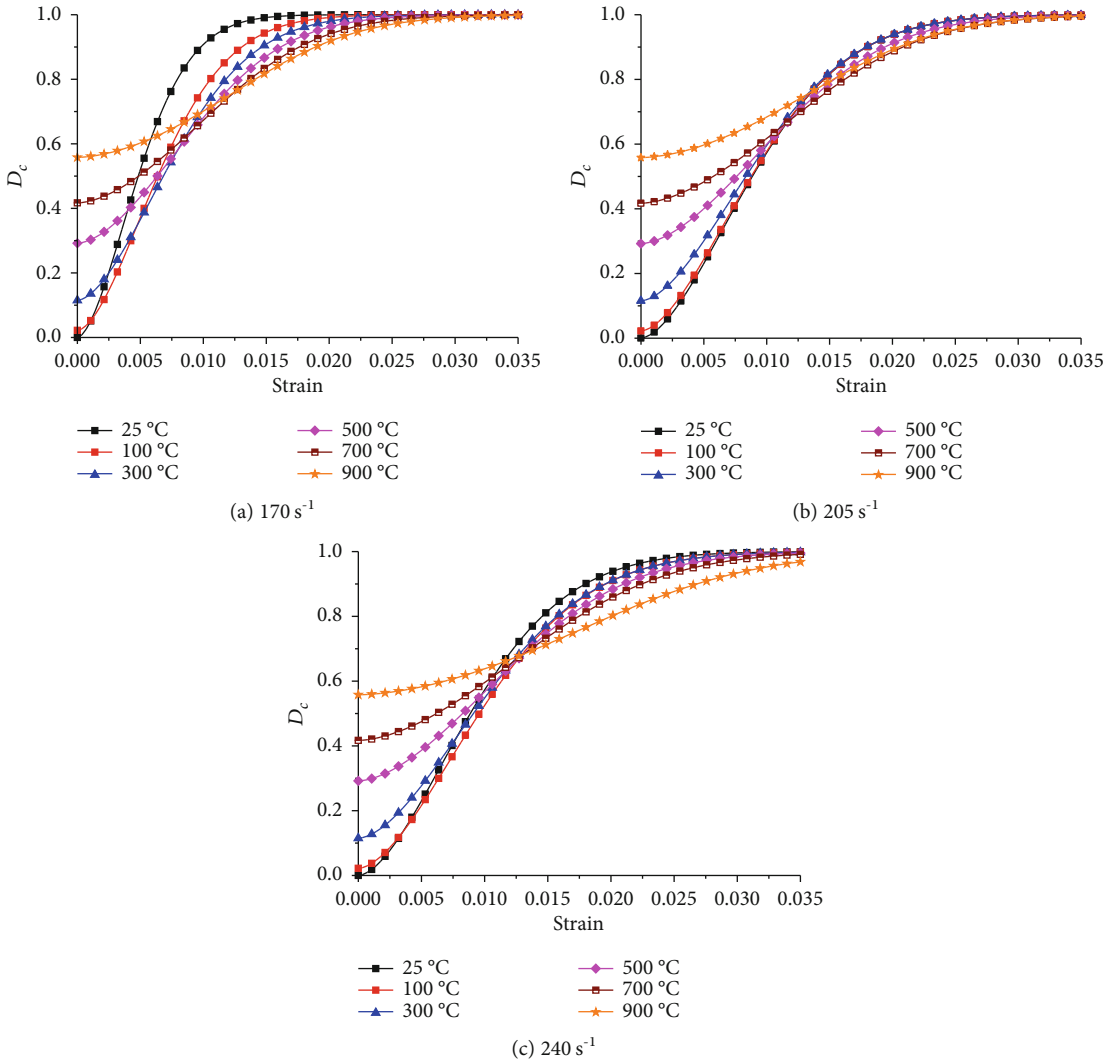

Figure 6: Dynamic damage growth curves of deep sandstone specimen with various temperatures.

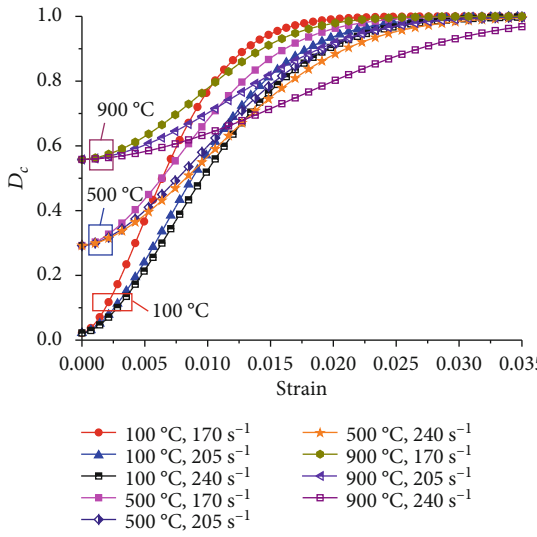

Figure 7: Dynamic damage growth curves of deep sandstone specimen with various strain rates.

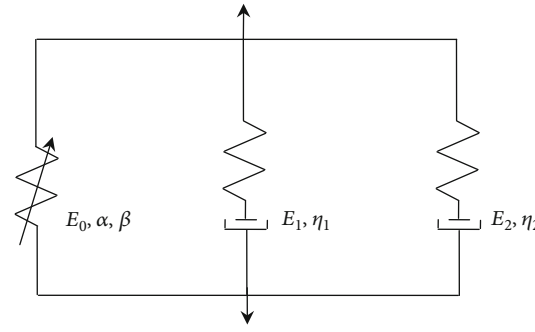

Figure 8: The ZWT model.

and deformation response of rock materials at high strain rate [38], as shown in Figure 8. It includes a nonlinear spring, a Maxwell element with low frequency, and a Maxwell element with high frequency. In addition, theoretical analysis indicates that the Maxwell element with low frequency has no enough time to relax, which will degenerate into a spring. Hence, the simplified ZWT model is expressed as

Table 2: The dynamic constitutive model parameters of deep sandstone.

Strain rate (s^{-1})	Temperature (°C)	λ	n	E_0 (GPa)	α (GPa)	β (GPa)	E_2 (GPa)	θ_2 (s^{-1})
170	25	0.006	1.7	60.3	-1.22×10^4	1.83×10^6	11.1	8.2×10^{-4}
	100	0.008	1.7	35.6	-1.13×10^2	2.55×10^5	7.7	8.5×10^{-4}
	300	0.009	1.7	39.2	-2.85×10^2	2.28×10^5	8.1	8.7×10^{-4}
	500	0.010	1.7	43.2	-3.99×10^2	1.83×10^5	7.9	8.2×10^{-4}
	700	0.011	1.7	42.2	-3.87×10^2	1.55×10^5	8.1	8.3×10^{-4}
	900	0.012	1.7	48.6	-4.92×10^2	1.81×10^5	7.3	8.4×10^{-4}
205	25	0.011	1.7	28.2	-1.07×10^2	1.58×10^5	7.9	8.3×10^{-4}
	100	0.011	1.7	31.5	-2.66×10^2	2.35×10^5	8.7	8.8×10^{-4}
	300	0.011	1.7	28.4	-1.16×10^2	1.38×10^5	8.1	8.9×10^{-4}
	500	0.012	1.7	40.5	-3.57×10^2	1.68×10^5	8.5	9.2×10^{-4}
	700	0.013	1.7	27.2	-1.38×10^2	6.29×10^4	8.1	7.8×10^{-4}
	900	0.013	1.7	23.9	-1.42×10^2	5.5×10^4	8.4	7.9×10^{-4}
240	25	0.011	1.7	62.9	-6.97×10^2	4.32×10^5	8.3	7.2×10^{-4}
	100	0.012	1.7	54.2	-5.29×10^2	2.88×10^5	8.3	8.9×10^{-4}
	300	0.012	1.7	45.3	-4.33×10^2	2.75×10^5	8.1	8.2×10^{-4}
	500	0.013	1.7	56.6	-4.89×10^2	2.23×10^5	7.8	8.6×10^{-4}
	700	0.013	1.7	34.8	-2.98×10^2	1.37×10^5	8.1	8.5×10^{-4}
	900	0.017	1.7	14.8	-2.18×10^1	7.87×10^3	8.2	8.1×10^{-4}

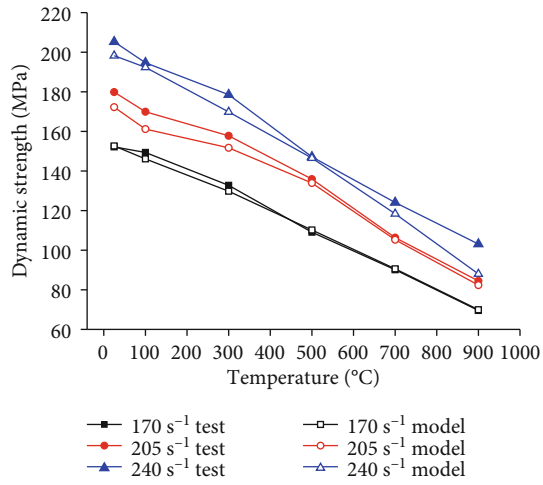

Figure 9: The comparison between theoretical and test dynamic strengths of deep sandstone specimen.

$$\sigma = E_0\varepsilon + \alpha\varepsilon^2 + \beta\varepsilon^3 + E_2\int_0^t \dot{\varepsilon}\ \exp\left(-\frac{t-\tau}{\theta_2}\right)d\tau, \quad (7)$$

where E_0, α, and β are elastic constants; E_1 and θ_1 are the elastic constant and relaxation time of low-frequency Maxwell element, respectively; E_2 and θ_2 are the elastic constant and relaxation time of high-frequency Maxwell element, respectively; t is the loading time; and τ is the time during stress wave.

A large number of previous theoretical and experimental results show that at high strain rate, the damage inside rock specimens is a gradual accumulation process [21]. Therefore, the damage evolution process should be considered in the simplified ZWT model:

$$\sigma = (1 - D_c)\left[E_0\varepsilon + \alpha\varepsilon^2 + \beta\varepsilon^3 + E_2\int_0^t \dot{\varepsilon}\ \exp\left(-\frac{t-\tau}{\theta_2}\right)d\tau\right]. \quad (8)$$

The dynamic damage constitutive model of deep sandstone can be obtained by substituting Equation (6) into Equation (8):

$$\sigma = \left\{\frac{(\nu_n/\nu_0)^2 \exp\left[-(\varepsilon/\lambda)^n\right]}{1 - \left[1 - (\nu_n/\nu_0)^2\right]\left\{1 - \exp\left[-(\varepsilon/\lambda)^n\right]\right\}}\right\} \cdot \left[E_0\varepsilon + \alpha\varepsilon^2 + \beta\varepsilon^3 + E_2\int_0^t \dot{\varepsilon}\ \exp\left(-\frac{t-\tau}{\theta_2}\right)d\tau\right]. \quad (9)$$

4.2. Verification of Dynamic Damage Compound Constitutive Model. The calculation method for parameters n and λ has been introduced in Section 3.2. The parameters of nonlinear spring (i.e., E_0, α, and β) control the shape of increasing stage of dynamic stress-strain curves. In addition, the approximate scope of E_2 and θ_2 can be estimated by subtracting two dynamic stress-strain curves of deep sandstone specimens under various strain rates [39]. The

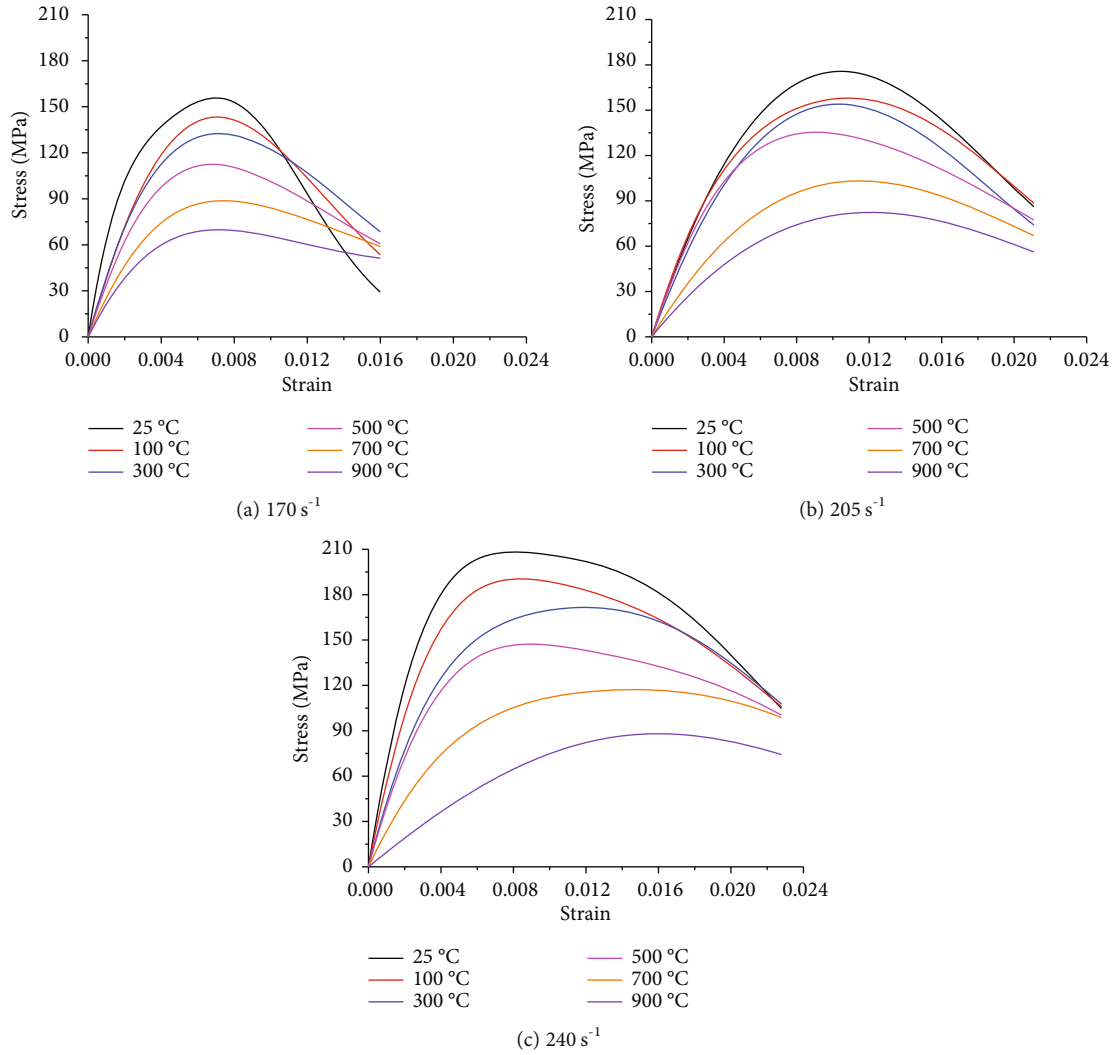

Figure 10: The theoretical dynamic stress-strain curves of deep sandstone specimen with various temperatures.

determined parameters for dynamic constitutive model are listed in Table 2. The comparison between theoretical and test dynamic strengths is shown in Figure 9. The theoretical dynamic stress-strain curves are shown in Figure 10. The above results demonstrate that the theoretical curves can well predict the weakening effect of high temperature on deep sandstone strength. Moreover, the effects of strain rate and temperature on dynamic strengths of deep sandstone specimen can be considered in the prediction results. However, the proposed theoretical results cannot well predict the experimental data in some test conditions.

5. Conclusions

(1) With the increase of high-temperature treatment, both the P-wave velocity and the dynamic strength of deep sandstone specimen decrease gradually, while its porosity increases and the variation rate of P-wave velocity and porosity accelerate after 300°C treatment

(2) With the increase of strain, the coupling damage of deep sandstone specimen gradually accumulates and presents "slow-fast-slow" three-stage characteristic. In addition, its growth rate decreases with the increase of thermal damage under various strain rates. With the increase of strain rate, the dynamic damage increase rate of deep sandstone specimen decreases gradually

(3) The dynamic constitutive model stress-strain curves are verified to provide well description of the dynamic strength and deformation behavior of deep sandstone under different high temperatures and strain rates. Moreover, the predicted values of dynamic peak strength with various conditions are found to essentially match the trends of laboratory data

Data Availability

The datasets generated and analyzed during the current study are available from the corresponding author on reasonable request.

Conflicts of Interest

The authors declare that there are no conflicts of interest regarding the publication of this paper.

Acknowledgments

This work is financially supported by the Natural Science Research Project of Colleges and Universities in Anhui Province (no. KJ2020A0296), Anhui Provincial Natural Science Foundation (no. 2008085QE220), National Natural Science Foundation of China (no. 52074005), and Doctoral Fund Project of Anhui University of Science and Technology (no. 13190025).

References

[1] F. Wang, T. Frühwirt, and H. Konietzky, "Influence of repeated heating on physical-mechanical properties and damage evolution of granite," *International Journal of Rock Mechanics and Mining Sciences*, vol. 136, article 104514, 2020.

[2] X. J. Hao, W. du, Y. X. Zhao et al., "Dynamic tensile behaviour and crack propagation of coal under coupled static-dynamic loading," *International Journal of Mining Science and Technology*, vol. 30, no. 5, pp. 659–668, 2020.

[3] Z. Zhongqiong, W. Qingbai, J. Guanli, G. Siru, C. Ji, and L. Yongzhi, "Changes in the permafrost temperatures from 2003 to 2015 in the Qinghai-Tibet Plateau," *Cold Regions Science and Technology*, vol. 169, article 102904, 2020.

[4] Z. W. Li, M. C. Long, X. T. Feng, and Y. J. Zhang, "Thermal damage effect on the thermal conductivity inhomogeneity of granite," *International Journal of Rock Mechanics and Mining Sciences*, vol. 138, article 104583, 2021.

[5] X. D. Zhang, E. C. Zhai, Y. Wu, D.'. Sun, and Y. T. Lu, "Theoretical and numerical analyses on hydro-thermal-salt-mechanical interaction of unsaturated salinized soil subjected to typical unidirectional freezing process," *International Journal of Geomechanics*, vol. 21, no. 7, article 04021104, 2021.

[6] Y. J. Wu, E. C. Zhai, X. D. Zhang, G. Wang, and Y. T. Lu, "A study on frost heave and thaw settlement of soil subjected to cyclic freeze-thaw conditions based on hydro-thermal-mechanical coupling analysis," *Cold Regions Science and Technology*, vol. 188, article 103296, 2021.

[7] H. du, F. Dai, M. D. Wei, A. Li, and Z. L. Yan, "Dynamic compression-shear response and failure criterion of rocks with hydrostatic confining pressure: an experimental investigation," *Rock Mechanics and Rock Engineering*, vol. 54, no. 2, pp. 955–971, 2021.

[8] M. Li, X. B. Mao, L. L. Cao, H. Pu, R. R. Mao, and A. H. Lu, "Effects of thermal treatment on the dynamic mechanical properties of coal measures sandstone," *Rock Mechanics and Rock Engineering*, vol. 49, no. 9, pp. 3525–3539, 2016.

[9] S. Huang and K. W. Xia, "Effect of heat-treatment on the dynamic compressive strength of Longyou sandstone," *Engineering Geology*, vol. 191, pp. 1–7, 2015.

[10] D. D. Ma, Q. Y. Ma, Z. M. Yao, and K. Huang, "Static-dynamic coupling mechanical properties and constitutive model of artificial frozen silty clay under triaxial compression," *Cold Regions Science and Technology*, vol. 167, article 102858, 2019.

[11] F. Q. Gong, Y. L. Wang, and S. Y. Wang, "The loading rate effect on the fracture toughness of marble using semicircular bend specimens," *Geofluids*, vol. 2020, Article ID 8876099, 8 pages, 2020.

[12] S. Gong, L. Zhou, Z. Wang, and W. Wang, "Effect of bedding structure on the energy dissipation characteristics of dynamic tensile fracture for water-saturated coal," *Geofluids*, vol. 2021, Article ID 5592672, 10 pages, 2021.

[13] L. Y. Yu, A. Fu, Q. Yin, H. W. Jing, T. Zhang, and G. Qin, "Dynamic fracturing properties of marble after being subjected to multiple impact loadings," *Engineering Fracture Mechanics*, vol. 230, article 106988, 2020.

[14] W. Yao, Y. Xu, W. Wang, and P. Kanopolous, "Dependence of dynamic tensile strength of Longyou sandstone on heat-treatment temperature and loading rate," *Rock Mechanics and Rock Engineering*, vol. 49, no. 10, pp. 3899–3915, 2016.

[15] S. Vidana Pathiranagei, I. Gratchev, and R. Kong, "Engineering properties of four different rocks after heat treatment," *Geomechanics and Geophysics for Geo-Energy and Geo-Resources*, vol. 7, no. 1, pp. 1–21, 2021.

[16] T. F. Chen, J. Y. Xu, S. Liu, P. Wang, and X. Y. Fang, "Experimental study on dynamic mechanical properties of post-high-temperature sandstone," *Explosion and Shock Waves*, vol. 34, no. 2, pp. 195–201, 2014.

[17] J. Y. Xu and S. Liu, "Effect of impact velocity on dynamic mechnaical behaviors of marble after high temperatures," *Chinese Journal of Geotechnical Engineering*, vol. 35, no. 5, pp. 879–883, 2013.

[18] H. M. Zhang, H. J. Xia, G. S. Yang et al., "Experimental research of influences of freeze-thaw cycles and confining pressure on physical-mechanical characteristics of rocks," *Journal of China Coal Society*, vol. 43, no. 2, pp. 441–448, 2018.

[19] L. F. Wang, T. R. Zeng, and Q. N. Weng, "Study on the constitutive model of saturated fine-grained sandstone based on statistical damage theory," *Materials Reports*, vol. 33, no. 11, pp. 3727–3731, 2019.

[20] R. L. Shan, Y. W. Song, L. W. Song, P. C. Haung, X. Dai, and T. Zhou, "Time dependent damage model of northwest artificial frozen red sandstone under dynamic loading," *Journal of China Coal Society*, vol. 43, no. 1, pp. 118–123, 2018.

[21] Y. X. Zhou, K. Xia, X. B. Li et al., "Suggested methods for determining the dynamic strength parameters and mode-I fracture toughness of rock materials," *International Journal of Rock Mechanics and Mining Sciences*, vol. 49, pp. 105–112, 2012.

[22] X. Li, W. Yao, and C. L. Wang, "The influence of multiple dynamic loading on fragmentation characteristics in dynamic compression tests," *Rock Mechanics and Rock Engineering*, vol. 54, no. 3, pp. 1583–1596, 2021.

[23] F. Q. Gong, H. Y. Jia, Z. X. Zhang, J. Hu, and S. Luo, "Energy dissipation and particle size distribution of granite under different incident energies in SHPB compression tests," *Shock and Vibration*, vol. 2020, Article ID 8899355, 14 pages, 2020.

[24] P. Xiao, D. Y. Li, G. L. Zhao, Q. Q. Zhu, H. X. Liu, and C. S. Zhang, "Mechanical properties and failure behavior of rock with different flaw inclinations under coupled static and dynamic loads," *Journal of Central South University*, vol. 27, no. 10, pp. 2945–2958, 2020.

[25] J. Y. Zhang, Y. J. Shen, G. S. Yang et al., "Inconsistency of changes in uniaxial compressive strength and P-wave velocity of sandstone after temperature treatments," *Journal of Rock Mechanics and Geotechnical Engineering*, vol. 13, no. 1, pp. 143–153, 2021.

[26] R. R. Zhang, D. D. Ma, Q. Q. Su, and K. Huang, "Effects of temperature and water on mechanical properties, energy dissipation, and microstructure of argillaceous sandstone under static and dynamic loads," *Shock and Vibration*, vol. 2020, Article ID 8827705, 13 pages, 2020.

[27] A. B. Jin, S. L. Wang, Y. D. Wei, H. Sun, and L. C. Wei, "Effect of different cooling conditions on physical and mechanical properties of high-temperature sandstone," *Rock and Soil Mechanics*, vol. 41, no. 11, pp. 3531–3539, 2020.

[28] J. Lemaitre, *A Course on Damage Mechanics*, Springer, New York, 1996.

[29] D. D. Ma, H. S. Xiang, Q. Y. Ma et al., "Dynamic damage constitutive model of frozen silty soil with prefabricated crack under uniaxial load," *Journal of Engineering Mechanics*, vol. 147, no. 6, 2021.

[30] J. Yu, W. Yao, K. Duan, X. Y. Liu, and Y. L. Zhu, "Experimental study and discrete element method modeling of compression and permeability behaviors of weakly anisotropic sandstones," *International Journal of Rock Mechanics and Mining Sciences*, vol. 134, article 104437, 2020.

[31] H. Yavuz, S. Demirdag, and S. Caran, "Thermal effect on the physical properties of carbonate rocks," *International Journal of Rock Mechanics and Mining Sciences*, vol. 47, no. 1, pp. 94–103, 2010.

[32] X. F. Li, Q. B. Zhang, H. B. Li, and J. Zhao, "Grain-based discrete element method (GB-DEM) modelling of multi-scale fracturing in rocks under dynamic loading," *Rock Mechanics and Rock Engineering*, vol. 51, no. 12, pp. 3785–3817, 2018.

[33] L. J. Zhou, S. L. Xu, J. F. Shan, Y. G. Liu, and P. F. Wang, "Heterogeneity in deformation of granite under dynamic combined compression/shear loading," *Mechanics of Materials*, vol. 123, pp. 1–18, 2018.

[34] Z. Rongrong, M. Qinyong, P. Qi, and M. Dongdong, "Effect of hydrothermal coupling on energy evolution, damage, and microscopic characteristics of sandstone," *High Temperature Materials and Processes*, vol. 39, no. 1, pp. 377–389, 2020.

[35] F. Q. Gong, X. F. Si, X. B. Li, and S. Y. Wang, "Dynamic triaxial compression tests on sandstone at high strain rates and low confining pressures with split Hopkinson pressure bar," *International Journal of Rock Mechanics and Mining Sciences*, vol. 113, pp. 211–219, 2019.

[36] Z. W. Yue, L. Z. Peng, X. L. Yue, J. X. Wang, and C. C. Lu, "Experimental study on the dynamic coalescence of two-crack granite specimens under high loading rate," *Engineering Fracture Mechanics*, vol. 237, article 107254, 2020.

[37] J. Yu, Z. H. Liu, Z. He, X. Q. Zhou, and J. B. Ye, "Fluctuation characteristic test of oblique stress waves in infilled jointed rock and study of the analytic method," *Advances in Civil Engineering*, vol. 2020, Article ID 7924742, 12 pages, 2020.

[38] G. M. Zhao, L. X. Xie, and X. R. Meng, "A constitutive model for soft rock under impact load," *Explosion and Shock Waves*, vol. 33, no. 2, pp. 126–132, 2013.

[39] D. D. Ma, Q. Y. Ma, and P. Yuan, "SHPB tests and dynamic constitutive model of artificial frozen sandy clay under confining pressure and temperature state," *Cold Regions Science and Technology*, vol. 136, pp. 37–43, 2017.